Experimental characterisation of the effects of thermal conditions on austenite formation for hot stamping of boron steel

Li, N.; Lin, J.; Balint, D.S.; Dean, Trevor

DOI:
10.1016/j.jmatprotec.2015.12.008

Title: Experimental Characterisation of the Effects of Thermal Conditions on Austenite Formation for Hot Stamping of Boron Steel

Author: N. Li J. Lin D.S. Balint T.A. Dean

PII: S0924-0136(15)30224-7
DOI: http://dx.doi.org/doi:10.1016/j.jmatprotec.2015.12.008
Reference: PROTEC 14655

To appear in: *Journal of Materials Processing Technology*

Received date: 27-4-2015
Revised date: 12-11-2015
Accepted date: 12-12-2015

Please cite this article as: Li, N., Lin, J., Balint, D.S., Dean, T.A., Experimental Characterisation of the Effects of Thermal Conditions on Austenite Formation for Hot Stamping of Boron Steel.Journal of Materials Processing Technology http://dx.doi.org/10.1016/j.jmatprotec.2015.12.008

Experimental Characterisation of the Effects of Thermal Conditions on Austenite Formation for Hot Stamping of Boron Steel

N. Li[a], J. Lin[a], D. S. Balint[a*] d.balint@imperial.ac.uk, T.A. Dean[b]

[a]Department of Mechanical Engineering, Imperial College London, London, SW7 2AZ, UK

[b]School of Mechanical Engineering, The University of Birmingham, Birmingham B15 2TT, UK

[*]Corresponding author: Tel: +44 (0) 207 594 7084

Highlights

1. Introduced a method to control microstructure and properties for hot stamped parts

2. Austenite formation in boron steel under a selective heating hot stamping process

3. Both full and intercritical austenite formation in boron steel were studied

4. Effects of heating rate, temperature, and time on transformation were quantified

5. Regularity demonstrated by the analysis can be used for materials modelling

Abstract

The formation of austenite in manganese-boron steels during selective heat treatment has great significance in the application of innovative hot stamping processes. Heat treatment tests were designed according to the thermal cycle of industrial heating and hot stamping processes and were conducted on a Gleeble 3800 thermomechanical testing system. Specimens were subjected to non-isothermal (heating rates: 1K/s–25K/s) and isothermal (soaking temperatures: 1023K–1173K) temperature profiles. A high-resolution dilatometer was employed to detect the dimensional change of the specimens associated with austenitization. The dilatometric measurement was quantitatively related to the volume fraction of austenite. By analysing the evolution curves of austenite fraction, the effects of heating rate and temperature on the progress of austenite formation under both non-isothermal and isothermal conditions were investigated and characterised, improving the current understanding of the mechanisms that control austenite formation in manganese-boron steels.

Keywords: Hot stamping; Boron steel; Tailored microstructure; Austenite formation; Heating conditions

Nomenclature

α : Ferrite

θ: Cementite

ψ: Parent phase of the studied steel

γ: Austenite

A_{e1}, A_{e3}: Temperature to start and complete austenite formation under equilibrium conditions

A_{c1}, A_{c3}: Temperature to start and complete austenite formation during continuous heating

W_0, W: Initial and instantaneous specimen width

ΔW: Change in specimen width

V_0, V: Initial and instantaneous specimen volume

v: Relative volume change

$v_{\psi 0}$, v_{ψ}(T): Relative volume change of the parent phase at 873K and at any temperature, respectively

$v_{\gamma 0}$, v_{γ}(T): Relative volume change of austenite at 873K and at any temperature, respectively

C_{ψ}, C_{γ}: Thermal expansion coefficient of the parent phase and austenite, respectively

f: Volume fraction of austenite

f_s: Saturated volume fraction of austenite

$\dot{N}$: Austenite nucleation rate

$\dot{G}$: Austenite growth rate

N_0, G_0, C: Pre-exponent parameters

Q_N, Q_G, Q_C: Activation energy

R: Gas constant

h: Heating rate

T: Absolute temperature (in Kelvin)

T_x: Temperature corresponding to certain volume fraction of austenite

e.g. $T_{50\%}$ is the temperature when volume fraction of austenite reaches 50%

t: Instantaneous time (origin: time at temperature of 873K)

t_{Ac1}: Time to start austenite formation (same origin as t)

t_x: Time corresponding to certain volume fraction of austenite (same origin as t)

e.g. $t_{80\%}$ is the time when volume fraction of austenite reaches 80%

Δt: Soaking time increment

$\Delta t_{x1\text{-}x2}$: Time to increase volume fraction of austenite from x1 to x2 during soaking

e.g. $\Delta t_{80\%f_s\text{-}90\%f_s}$ is the time to increase volume fraction of austenite from 80% of f_s to 90% of f_s during soaking

$\Delta t'$: Time increment during continuous heating

$\Delta t'_{Ac1\text{-}x}$: Time increment from starting austenite formation to reaching certain volume fraction of austenite during continuous heating

1. Introduction

The rising demand for increased safety and reduced weight of car bodies has stimulated technological innovation in sheet metal forming. According to Karbasian and Tekkaya (2010), hot stamping of boron steel in order to obtain lightweight, strong components is now a well developed process. In the process blanks are austenitized then formed and quenched in cold dies so that ultra-high strength parts in the martensite phase are obtained. Currently, great attention is being paid to improving the process to produce parts with tailored distributions of mechanical properties, allowing parts to be made that conform more fully to functional requirements. For example, in safety critical beams in automobiles, instead of utilising a fully martensite phase, regions of ductile phases, such as ferrite and pearlite, can be incorporated to enhance energy absorption or tune crash deceleration pulses; this concept is described in a patent by Thomas and Detwiler (2009) on optimizing structural performance by microstructural design, which can be realized by controlling thermal conditions during forming. As a result, comprehensive studies have been carried out on the phase transformation behaviour of boron steels during cooling, such as the experimental characterisation of cooling rate effects (Gárlipp et al., 2001), and modelling of austenite decomposition (Åkerström and Oldenburg, 2006). This knowledge could be applied to selective quenching in hot stamping. However, because a long cooling time is required to achieve ductile phases, there is an intrinsic conflict with the industrial requirement for short cycle times. Therefore, a novel strategy for selective heating of boron steels has been proposed by the authors (Li et al., 2012; Li et al., 2014): A blank is heated under tailored thermal conditions, which enables part of the steel to be fully or partially austenitized with the remainder experiencing no phase transformation. Subsequently, the blank is formed and rapidly quenched in cold dies as in conventional hot stamping operations. The fraction and distribution of martensite in the formed part is determined by the extent of austenitization.

Hence the formation of austenite during the heating process is of primary importance in determining the final properties of a given part. Therefore understanding the kinetics of austenite formation is essential in optimizing the design of the heat treatment conditions for innovative hot stamping processes.

Studies on austenite formation have been carried out by many researchers. Roberts and Mehl (1943) established the nucleation and growth character of the transformation in steels with different starting microstructures. However, compared with the number of investigations into decomposition of austenite during cooling, studies on austenite formation have been few. As stated by Reed et al. (1998) and Schmidt et al. (2007), this is primarily because it is difficult to retain austenite at room temperature for inspection and characterisation, which makes observation of the progress of austenite formation difficult. Stimulated by automotive applications, the development of advanced high strength steels has recently revived interest in the heating stage of the heat treatment cycle. Initially, attention was focused on partial austenite formation in intercritical annealing practices, since this offers a means of optimizing the mechanical properties of dual-phase steels. More extensive and systematic research on the formation of austenite has been conducted during the last decade, in order to achieve quantitative understanding of microstructural evolution during transformation and the mechanisms that control it under different conditions. For example, Asadi Asadabad et al. (2008) characterised the relationship between temperature and time of intercritical annealing and transformed fraction of austenite in dual phase steels; Oliveira et al. (2007) investigated the effects of heating rates on critical temperatures of austenite formation in a low carbon steel. However, information on austenite formation in boron steels for hot stamping applications is still limited; Cai (2011) focused on only full austenite formation under continuous heating conditions. Little research has been carried out on the intercritical soaking of boron steels. In addition, the influence of temperature and heating rate on the progress of

the transformation to austenite has always been studied separately under isothermal conditions and non-isothermal, respectively. In a real situation, the conditions for work-piece preheating for hot pressing are first increasing temperature followed by steady-state temperature. This should be recognised if an accurate evaluation of austenite evolution is to be obtained.

As stated by Thibaux et al. (2007), formation of austenite is a diffusion-controlled process and is primarily determined by the initial microstructure of the material. In this study, the kinetics of austenitization is assumed to be mainly a carbon diffusion-controlled process. This is because the diffusivity of carbon in steel is nearly $10^5 – 10^6$ times greater than that of substitutional solutes (e.g. Mn), as reported by Khaira et al. (1993). Therefore, for hot stamping of boron steels in industrial applications, within the practical soaking time, the establishment of equilibrium is with respect to carbon without taking substitution solutes into account. As the carbon content is in the range of 0.02 wt.% – 0.76 wt.%, the boron steel studied here is a hypoeutectoid steel. Figure 1 (a) schematically illustrates the phase composition of a hypoeutectoid steel prior to (a-1), during (a-2), and upon completion of austenitization (a-3). The austenite formation in a hypoeutectoid steel proceeds in two stages. Firstly, from the research results by Caballero et al. (2000), austenite nucleation takes place at the interfaces of ferrite-cementite lamellae within a colony, as well as at the intersections or interfaces of pearlite colonies. The new grains of austenite grow into pearlite colonies to replace the eutectoid ferrite; at the same time, the cementite dissolves in the austenite. Secondly, from the research results by Jacot and Rappaz (1999), the reaction proceeds into the remaining pro-eutectoid ferrite. The transformation from pro-eutectoid ferrite to austenite is enabled by the diffusion of carbon atoms from inside the enriched γ grains to γ/α interfaces, so that the γ/α interfaces gradually move towards α phase regions. This process continues until the average carbon content in the austenite becomes equal to the carbon content of the

steel. This phase transformation is a thermodynamic process and significantly depends upon the thermal conditions of heat treatment. The Fe-C equilibrium diagram (solid line) for the proeutectoid part (0.02 wt.% < C% < 0.76 wt.%) is given in Figure 1(b). A_{e1} and A_{e3} are the starting and finishing temperatures of austenite formation for a proeutectoid steel in the equilibrium state. If the steel is soaked at a temperature between A_{e1} and A_{e3}, which is termed the intercritical region, only partial austenitization can be achieved, which has been proved by the studies of Yi et al. (1985) and Asadi Asadabad et al. (2008). The equilibrium state is a mixture of austenite and ferrite phases ($\alpha + \gamma$). For most practical hot forming applications, the preheating of steel is continuous. The austenite formation in boron steel generally involves heating the material through the two-phase region ($\alpha + \gamma$) into the single austenite phase region (γ). In this condition, the starting and finishing temperatures of the transformation do not follow the equilibrium diagram anymore. According to the investigation by Garcia de Andrés et al. (2002), they are shifted to higher temperatures, called A_{c1} and A_{c3}, which are sensitive to the heating rate. Therefore, as shown in Figure 1(b), the phase diagram is modified for transformations that occur under continuously increasing temperature conditions. The evolution of material microstructure (given in Figure 1(a)) is illustrated in the phase diagram accordingly.

In this work, the formation of austenite in a manganese-boron steel under both continuous heating and isothermal soaking conditions, which are designed according to the thermal cycle of selective heating for hot stamping processes, is investigated through dilatometry and theoretical analysis. The main aim of the paper is to gain a better understanding of the kinetics of the austenite formation in boron steels, and evaluate the influence of heating rate and soaking temperature on the process.

2. Experimental procedure

The material used in this study was a 22MnB5 manganese-boron steel from ThyssenKrupp Steel. The supplier provided the following product information: the chemical composition of the steel is listed in Table 1; the initial microstructure contained an approximate 78%/22% mixture of proeutectoid ferrite and pearlite.

A dilatometer was used to measure the width change (ΔW) of the specimen during thermal cycles, from which the phase transformation can be characterised. Experiments were carried out using a Gleeble 3800 thermomechanical testing system which enables accurate process control and has the capability for phase transformation to be monitored using a high-resolution dilatometer. Rectangular specimens, with K-type thermocouples fixed in the middle, were used for the tests. They were cut from the same piece of cold rolled 1.6mm thickness sheet. The initial gauge length of the specimen was 20mm and the width (W_0) was 10mm.

The heat treatment conditions, performed on the Gleeble machine, were designed to match the thermal cycle used in practice for hot stamping of boron steels, which consists of continuous heating, isothermal soaking and quenching, as shown in Figure 2. Starting from a given initial microstructure, the heating rate and soaking temperature are the two critical factors which affect the kinetics of austenitization. In order to study the effects of these parameters under both non-isothermal and isothermal conditions, two groups of testing programmes were designed. In the first group, specimens were heated to 1173K at different heating rates from 673K; 1173K is the soaking temperature adopted for full austenitization in hot stamping practice for this boron steel, as established by Li et al. (2014). Long soaking periods were applied to ensure complete austenite phase transformation. The soaking period was 10 minutes for the 1K/s heating rate and 15 minutes for the 5K/s and 25K/s heating rates. In the second group, specimens were heated at a rate of 5K/s to different soaking

temperatures of 1023K, 1073K, 1123K, and 1173K, and held for 15 minutes to enable austenite formation. After the heating and soaking periods, all specimens were quenched at a cooling rate of 50K/s, which ensured complete transformation from austenite phase to martensite phase, per the results of Li et al. (2012). The critical cooling rate for martensite transformation from austenite is 27K/s, according to the material supplier.

3. Dilatometric results and analysis

When a material undergoes a phase transformation, the lattice structure changes, which is in principle accompanied by a change in specific volume. The formation of austenite involves the lattice change of iron from a body-centred cubic (BCC) structure to a face-centred cubic (FCC) structure, which results in a change in density, hence volume. The evolution of austenitization can thus be deduced from the experimental results of dilatometry, which has been introduced and applied in previous studies by Garcia and Deardo (1981) and Reed et al. (1998).

3.1 Dilatometric curves

Figures 3 (a) and (b) show the experimentally measured width change (ΔW) versus temperature and time, respectively. The test was carried out at a heating rate of 5 K/s with a soaking temperature of 1173K for 15 minutes. The experimental curve can be divided into four stages. As can be seen in Figure 3 (a), in the first stage, the dilatometric curve exhibits a linear expansion as the temperature increases. This is a pure thermal expansion of the boron steel with initial phase mixture. In the second stage, the dilatometric curve deviates from linearity at 1007K (A_{c1}). This is because the formation of austenite takes place, which contributes to the change of the specimen width. For the continuous heating stage, the curve is a result of the competition between the volumetric change induced by phase transformation and thermal expansion. For the isothermal soaking stage, the curve only shows contraction caused by the phase transformation (the vertical part in Stage 2 shown in Figure 3(a)). As

shown more clearly in Figure 3 (b), the austenite transformation rate in the isothermal soaking period decreases with the soaking time. After 15 minutes of soaking time (Figure 3(b)), the rate of change of the width tends to zero, i.e. $d(\Delta W)/dt \approx 0$. It can be concluded that thermodynamic equilibrium has been achieved. (Note: as explained earlier, the term 'equilibrium' in this study refers to the constrained equilibrium with respect to carbon, which suits the hot stamping conditions.) The microstructure ends up being entirely austenite γ for this case, since the soaking temperature is above A_{e3}. The final microstructure could be a mixture of austenite and ferrite (γ + α) if the soaking temperature is between A_{e1} and A_{e3}. In the third stage, the curve is linear again, which reflects the pure thermal contraction of the steel during quenching or rapid cooling. In the fourth stage, volume expansion is shown on the curve, which corresponds to the phase transformation from austenite γ to martensite α'. Since this study is mainly concentrated on the formation of austenite, the analysis is focused on the experimental data in Stage 2 of Figure 3. The experimental results, corresponding to the period from 873K to the end of soaking, under different testing conditions are summarised in Figure 4. The data presented for each condition was averaged over 3 repeats.

Figure 4 (a) shows the width changes of specimens (ΔW) with temperature and time, respectively, for different heating rates and a constant soaking temperature of 1173K. During the continuous heating period (the left figure) a lower starting temperature (A_{c1}) and more contraction of width due to austenitization are observed for the lower heating rate. During the isothermal soaking period (the right figure) the width change (ΔW) for all heating rates reduces gradually and becomes constant at a common value. This indicates that, given sufficient soaking time, the austenite formation could be completed at the temperature of 1173K. Note, this is higher than A_{e3}. Thus, the austenite formation has been completed for all three of the tests. Figure 4 (b) again shows ΔW of specimens with temperature and time. However these tests were carried out at a heating rate of 5K/s and held at 4 different soaking

temperatures of 1023K, 1073K, 1123K and 1173K for 15 minutes. During the continuous heating period (the left figure), ΔW for all tests almost lies on the same curve as the heating rate was common to all of them. During the isothermal soaking period (the right figure) all the curves tend to become horizontal eventually, which shows thermodynamic equilibrium has been virtually reached for every isothermal soaking condition. A different reduction of ΔW can be seen for each of the soaking temperatures; however, the value of the width change (ΔW), is a function not only of phase composition but also instantaneous temperature and therefore is not an indicator of the degree of phase transformation alone.

3.2 Calculation of austenite volume fraction

A transformation method has been developed and explained below for the calculation of austenite volume fraction based on the experimentally measured ΔW. Referencing the true strain definition, the relative volume change v during the thermal-expansion/contraction and phase transformation can be expressed as:

$$v = \ln \frac{V}{V_0} \tag{1}$$

where V_0 is the initial volume of the specimen, and V is the volume at any time during the thermal cycle.

Assuming that the specimen expands isotropically, i.e. $v = W^3$, the relative volume change can thus be related to ΔW as follows:

$$v = 3\ln \frac{W}{W_0} = 3\ln(\frac{\Delta W}{W_0} + 1) \tag{2}$$

Based on Equation (2), the width change curve, shown in Fig 3 (a), can be converted to a relative volume change curve, as shown in Figure 5.

Regarding the pure thermal expansion and contraction stages, the following relationship is proposed:

$$v_\psi(T) = v_{\psi 0} + C_\psi \Delta T; \quad v_\gamma(T) = v_{\gamma 0} + C_\gamma \Delta T \tag{3}$$

where $v_{\psi 0}$ and $v_\psi(T)$ are the relative volume change of the parent phase (ferrite and pearlite mixed microstructure, represented by ψ in this study) at 873K and any temperature T, respectively. $v_{\gamma 0}$ and $v_\gamma(T)$ are the relative volume change of the austenite phase (γ) at 873K and any temperature T, respectively. ΔT is the temperature increment from 873K. C_ψ and C_γ are the thermal expansion coefficients of the material with the initial phase mixture and austenite, respectively. Corresponding to the slopes of the linear regions in Figure 5, they have been measured as: $C_\psi = 4.41056 \times 10^{-5}$ K^{-1} and $C_\gamma = 6.82215 \times 10^{-5}$ K^{-1}.

Regarding the phase transformation stage, the relative volume change, which is a function of both temperature and time, can be given as:

$$v(T,t) = (1-f)v_\psi(T) + f\, v_\gamma(T) \tag{4}$$

where f is the volume fraction of austenite. Thus the extent of phase transformation can be calculated as:

$$f = \frac{v_\psi(T) - v(T,t)}{v_\psi(T) - v_\gamma(T)} \tag{5}$$

where $v_\psi(T)$ and $v_\gamma(T)$ are calculated according to equation (3), and $v(T, t)$ is obtained from the relative volume change-temperature curve in Figure 5. Based on Equations (2), (3) and (5), the dilatometric curves shown in Figure 4 can thus be presented in terms of austenite volume fraction, as shown in Figure 6 (the volume fractions are multiplied by 100%). This permits a more rational insight into the progress of austenite formation.

Figure 6 (a) shows the first group of test results. The austenite formation progresses differently during continuous heating for different heating rates. When the continuous heating ends at 1173 K, the amount of transformed austenite depends on the heating rate: for 1K/s, f = 77%; for 5K/s, f = 61%; and for 25K/s, f = 54%. Subsequently, the volume fractions of austenite (f) keep increasing to roughly 100% at different rates under isothermal conditions

despite the soaking temperature being the same. Figure 6 (b) shows the second group of tests. With increasing soaking time, the volume fraction of austenite (*f*) increases and then becomes almost constant at a value less than 100%, which depends on soaking temperature. The maximum value of volume fraction obtained for each soaking temperature is: for 1023K, f = 32%; for 1073K, f = 83%; for 1123K, f = 92%; and for 1173K, f = 99%.

4. Discussion and analysis

The phase transformation in general is controlled by two classes of factors: 1) Initial microstructure, including phase composition, chemical composition, grain size and the presence of non-metallic inclusions; that is, the intrinsic properties of an alloy. 2) External conditions, including heating rate and temperature. Assuming that the intrinsic properties of the tested boron steel were to the supplier's specification and the same for all specimens, this study quantifies the effects of process conditions; heating rate and soaking temperature on the progress of austenite formation.

4.1 Full austenite formation

The first group of tests, shown in Figure 6 (a), are used to investigate the effects of heating rate on the austenite formation. In these tests, the specimens experienced different heating rates to a constant temperature of 1173K (above A_{e3}) and were held for 10-15 minutes, which enabled the material to be fully transformed to austenite. The austenite formation features for the material are studied in the heating and isothermal soaking conditions separately, as follows:

4.1.1 Effects of heating rate on non-isothermal austenite formation

It is stated in Section 1 that particular amounts of superheating above the equilibrium temperatures A_{e1} and A_{e3} are required to start and complete the phase transformation under

non-isothermal conditions. The temperatures and times to start austenite formation (defined as when f = 2% in this study) and to attain a particular volume fraction of austenite (f = 10% to 50%) in the heating stage, as measured for different heating rates, are summarized in Figure 7(a), which is normally called a continuous heating transformation (CHT) diagram. It is apparent that less time is required at a higher heating rate to achieve the same volume fraction of austenite. Savran (2009) has reported that during continuous heating, a higher heating rate stimulates a higher nucleation rate, which allows more nuclei for austenite formation to be generated even within a shorter period of time, thus enabling a higher overall growth rate of austenite. Figure 7(a) also shows that the starting temperature A_{c1} increases with increasing heating rate. For example, at the heating rate of 1K/s, the temperature for A_{c1} is 1000K, but for the heating rate of 25K/s it is 1114K. The same phenomenon can be observed for the other volume fractions (f = 10% to 50%) shown in Figure 7(a) that the temperature to attain a particular amount of austenite increases with increasing heating rate. This is mainly because a higher heating rate means less soaking time is available for diffusional transformation with a given growth geometry and the transformation would be shifted to higher temperatures, which was also reported by Huang et al. (2004) and Cai (2011). The quantification of the heating rate effects on austenitization under continuous heating conditions is complex, since heating rate is coupled with both temperature and time. To facilitate the characterisation, the testing data was re-processed in terms of Figure 7 (b) and (c).

Figure 7 (b) shows that the relationship between heating rate and temperature for a particular volume fraction of austenite formation (f = 0% to 50%) is linear on a log-log scale. In the equations given for the trend lines, h is heating rate in K/s, and T is the abso;lute temperature in K. For example, for 50% austenite formation, the 3 data points of the temperature and heating rate can be approximated by $T_{50\%}=1084h^{0.018}$ (the top line in Figure 7(b)). The slopes

of the trend lines for different volume fractions are positive and increase with increasing austenite volume fraction. For example, for f = 10%, the slope is 0.006, and for f = 50%, the slope is 0.018. This is because the shift to higher temperatures due to insufficient time for diffusional transformation becomes greater as the transformation proceeds. Figure 7 (c) shows the relationship between heating rate and the required time for particular volume fractions of austenite formation. The trends are again linear on a log-log scale. The heating time increment, $\Delta t'$, is the time elapsed from the start of austenite formation to the time at which a particular volume fraction of austenite (f = 10% to 50%) is attained. For example, $\Delta t'_{\text{Ac1-50\%}}$ is the time elapsed from the temperature A_{c1} to the time when f reaches 50%. The slopes of the trend lines are negative, which again reveals that the transformation time for a certain volume fraction of austenite decreases with increasing heating rate. The magnitude of the trend slope decreases with increasing austenite volume fraction, which indicates that the effect on transformation time is weakened as the transformation proceeds.

The linear features shown in Figure 7 (b) and (c) provides useful information for the modeling of austenite formation. Nucleation and growth are the two primary mechanisms operating in the phase transformation process. Referring to the studies of Liu et al. (2007), it is proposed to model their rates using the equations of:

$$\dot{N} = N_0 \exp\left(-\frac{Q_N}{RT}\right) \tag{6}$$

$$\dot{G} = G_0 \exp\left(-\frac{Q_G}{RT}\right) \tag{7}$$

where R is the gas constant and T is the absolute temperature; Q_N and Q_G are the activation energies for nucleation and growth, respectively; N_0 and G_0 are pre-exponential factors which can be functions representing the effects of influencing factors on nucleation and growth. According to the analysis in this work, heating rate as a critical thermodynamic factor should also be taken into account in non-isothermal austenite formation. Therefore, with respect to

the formulae for N_0 and G_0, in addition to the material related parameters, it is suggested that heating rate should be incorporated in terms of a power law.

4.1.2 Effects of heating rate on isothermal austenite formation

Figure 8 shows the required time to increase austenite volume fraction by 5% at different stages (f = 80%, 85%, and 90%) of the isothermal transformation for different heating rates. The isothermal transformation takes place at a constant soaking temperature of 1173K, at which full austenite formation is achievable. The soaking time increment, Δt, is the time elapsed from attaining a particular austenite volume fraction (f) to the time at which a different, higher value of f is attained during soaking. For example, $\Delta t_{80\%\text{-}85\%}$ is the time elapsed from f = 80% to f = 85%. It can be seen, again, that the relationship between heating rate and soaking time increment is linear on a log-log scale. Similar to Figure 7 (c), the slopes of the trend lines are negative. This reveals that, at the same stage of the transformation under the same isothermal condition, less time is required for higher heating rates. This is consistent with the trend found in an Fe-C-Mn-Mo steel studied by Huang et al. (2004). The phenomenon leads to the important conclusion that the thermodynamic effect of the heating rate proceeds from the heating step and continues through the subsequent isothermal soaking step. This is because the transformation rate at any time depends on both the instantaneous growth rate of new phase grains and the existing quantity of the grains (not just the instantaneous nucleation rate), which has been detailed by Liu et al. (2007). As discussed earlier, since more nuclei are generated during continuous heating at a higher rate, during the subsequent isothermal soaking at a given temperature, a larger amount of pre-existing grains enables a higher overall growth rate of new phase, i.e. a higher austenite formation rate. It can be observed that all the trend lines in Figure 8 are nearly parallel. This interesting feature indicates that the influence of heating rate on the isothermal transformation remains constant

throughout the different austenite formation stages. Moreover, another feature shown in Figure 8 is that a longer time is required to increase the austenite volume fraction by 5% at a later stage of the transformation, which reveals the impingement mechanism in the steel. As described by Lenel (1983), towards the end of the reaction when a large amount of austenite has been formed, impingement of neighbouring growth centres (or their diffusion fields) will occur, which slows down the reaction rate and increases the time taken to reach equilibrium.

The evolution curves of austenite volume fraction, corresponding to a period of 10 minutes starting from isothermal soaking, for each of the three testing conditions, are plotted versus normalised time in Figure 9. In Figure 9 (a), the normalised time is given by $(t\text{-}t_{80\%})/\Delta t_{80\%–85\%}$, where t is measured relative to the time at which 873K is attained, $t_{80\%}$ is the time t for f = 80% and $\Delta t_{80\%–85\%}$ is the transformation time to increase austenite volume fraction by 5% from 80%; the time for f = 80% is the origin on the horizontal axis. It is required of this normalisation that the influence of temperature and heating rate be constant throughout the austenitization process. With this time normalization, the features of an austenite volume fraction evolution curve should be determined only by the metallurgical properties that control the transformation kinetics, i.e. the dependency on temperature and heating rate should be eliminated. As shown in Figure 9 (a), the evolution curves of austenite volume fraction for different heating rates collapse onto a single curve, which saturates as time progresses, when time is normalised in this way. This indicates that the impingement mechanism in the isothermal transformation stage does not depend on the heating conditions in the range that was considered. It can also be noted from Figure 9 (a) that the curve with the highest heating rate, 25K/s, is closer to equilibrium than the other heating rate curves at the same transformation time despite starting with the lowest volume fraction of austenite. This again shows that a higher heating rate enables a higher rate of subsequent isothermal transformation. To confirm this regularity, normalisation is made using two different time

scales. In Figures 9 (b) and (c), the times for f = 85% and f = 90% are taken as the origins of the horizontal axis, respectively, and the soaking time increments $\Delta t_{85\%–90\%}$ and $\Delta t_{90\%–95\%}$ are used as the respective normalisation factors. The same features shown in Figure 9 (a) can be observed in Figures 9 (b) and (c). The only difference is the normalised time scale; the value of the normalisation factor Δt is larger at later stages of the transformation as shown in Figure 8. Figure 9 indicates that the effect of heating rate on austenite formation can be eliminated if the transformation time is normalised using the method introduced here.

4.2 Intercritical annealing

In the second group of tests, the specimens were heated at the same rate of 5K/s to different temperatures (1023K, 1073K, 1123K and 1173K), and then held at these respective temperatures for sufficient time (15 minutes) to achieve an equilibrium condition of austenite at each temperature. This provides insight into the kinetics of austenite formation during isothermal soaking at intercritical temperatures.

4.2.1 Saturated volume fraction

At an intercritical temperature between A_{e1} and A_{e3}, full formation of austenite cannot be achieved. In this work, the value of austenite volume fraction that can ultimately be achieved at any given soaking temperature, T, is termed as the saturated volume fraction f_s. Referring to the austenite formation and saturation features shown in Figure 6 (b), the saturated austenite volume fractions can be obtained for different soaking temperatures (between A_{e1} and A_{e3}, or above A_{e3}), as shown in Figure 10. The experimental result for f_s plotted against T has a sigmoidal form. It can be concluded that, for the studied boron steel, the temperatures A_{e1} is a value between 973K and 1023K, and A_{e3} is a value between 1123K and 1173K.

According to the analysis in section 4.1, it is also known that, although heating rate affects the austenite transformation rate, it doesn't affect the maximum obtainable value of austenite fraction at a particular soaking temperature, i.e. f_s is only a function of temperature. This is consistent with existing studies on dual-phase steels conducted by Yi et al. (1985) and Asadi Asadabad et al. (2008).

4.2.2 Effects of temperature on isothermal austenite formation

Figure 11 shows the transformation time for an increase in austenite volume fraction of 10% of f_s relative to 80% of f_s (i.e. $f = 80\%f_s - 90\%f_s$) for different soaking temperatures. Again, Δt is the soaking time increment and $\Delta t_{80\%fs\text{-}90\%fs}$ is the time elapsed from f equal to 80% of f_s to f equal to 90% of f_s. It can be seen that less transformation time is required at a higher temperature; in addition, the relationship between the logarithmic soaking time increment, $\ln(\Delta t)$, and inverse temperature, $1/T$, approximately follows a straight line, which can be described by:

$$\Delta t = C \exp\left(\frac{Q_C}{RT}\right) \tag{8}$$

where C is a material constant, Q_c is an activation energy, R is the gas constant and T is absolute temperature. Referring to the research results by Savran (2009), the regularity can be explained as follows: in the steel studied here, it can be expected that the nucleation of austenite occurs only in pearlite colonies and all the nucleation sites are consumed quickly at the beginning of the transformation. Thus, having the same heating rate, the same amount of nuclei should be generated in the tests. Then, the transformation rate is controlled by only the growth rate of the austenite phase. Thus, it is determined by only the soaking temperature under isothermal conditions. This is the reason that, considering transformation time and rate are in inverse proportion, that Equation (8) is consistent with Equation (7).

The austenite volume fractions evolving over a period of 10 minutes starting from 80% of f_s are plotted for each of the four soaking temperatures versus the normalised time (t-$t_{80\%fs}$)/$\Delta t_{80\%fs\text{-}90\%fs}$ in Figure 12 (a). The rates of austenite formation for the different cases within the same time period are illustrated, which again indicate that a higher soaking temperature enables faster progress towards equilibrium. In Figure 12 (b), the austenite volume fraction is normalised by f_s of the corresponding soaking temperature. Similar to Figure 9, the trends are nearly identical, which reveals that the isothermal austenite formation at different intercritical temperatures obeys the same kinetics of growth and impingement as equilibrium is approached.

5. Conclusions

According to the analysis of the experimental results, the following conclusions can be drawn about austenite formation in the boron steel studied here:

- During the heating stage, at a higher heating rate, less time and a higher temperature are required to attain a certain volume fraction of austenite. Both temperature and time follow linear relationships with heating rate in logarithmic coordinates. The effects of heating rate are greater on temperature than time for a larger amount of austenite formation.
- The influence of heating rate is at the same level in the subsequent isothermal step. The times to attain particular volume fractions of austenite (80%–85%, 85%–90% and 90%–95%) are linearly related to heating rate in logarithmic coordinates. During soaking, equilibrium can be approached in less time when the heating rate is higher.
- For austenite formation under intercritical soaking, equilibrium can be approached in less time when the temperature is higher. The logarithm of time to attain a particular

percentage of saturated austenite volume fraction, 80%f_s–90%f_s at a chosen temperature, follows a linear relationship with inverse temperature.

- Regarding isothermal austenite formation, following a given heating rate or temperature, all evolution curves of normalised austenite volume fraction (f/f_s) follow the same trend line approaching equilibrium when plotted on a normalised time scale. (f_s is 100% for full austenite formation.) This shows that the mechanisms controlling transformation do not change with conditions in the range of heating rate and temperature considered.
- The characterisation of the dynamics of the austenite formation process is essential for the thermal condition design, e.g. heating rate and soaking temperature, to enhance productivity and reduce energy consumption in hot stamping processes. The optimization of thermal conditions can benefit further by modelling the austenite formation based on this study. The data, regularity, and insights obtained by the analysis can provide useful information for materials modelling, in terms of formulation of equations, quantification of influencing parameters, and determination of material constants.

Acknowledgements

The authors thank SAIC Motor UK Technical Centre for financial support and the supply of MBW manganese-boron steel.

References

Åkerström, P., Oldenburg, M., 2006. Austenite decomposition during press hardening of a boron steel—Computer simulation and test. Journal of Materials Processing Technology 174, 399-406.

Asadi Asadabad, M., Goodarzi, M., Kheirandish, S., 2008. Kinetics of austenite formation in dual phase steels. ISIJ International 48, 1251–1255.

Caballero, F.G., Capdevila, C., Garcı´a de Andre´s, C., 2000. Influence of scale parameters of pearlite on the kinetics of anisothermal pearlite to austenite transformation in a eutectoid steel. Scripta mater. 42, 1159–1165.

Cai, J., 2011. Modelling of phase transformation in hot stamping of boron steel, Mechanical Engineering. Imperial College London.

Garcia, C.I., Deardo, A.J., 1981. Formation of austenite in 1.5 pct Mn steels Metallurgical Transactions A 12A, 521-530.

Garcia de Andrés, C., Caballero, F.G., Capdevila, C., Álvarez, L.F., 2002. Application of dilatometric analysis to the study of solid–solid phase transformations in steels. Materials Characterization 48, 101-111.

Gárlipp, W., Cilense, M., Novaes Gomes, S.I., 2001. Austenite decomposition of C–Mn steel containing boron by continuous cooling. Journal of Materials Processing Technology 114, 71-74.

Huang, J., Poole, W.J., Militzer, M., 2004. Austenite formation during intercritical annealing. Metallurgical and Materials Transactions A 35, 3363-3375.

Jacot, A., Rappaz, M., 1999. A combined model for the description of austenitization, homogenization and grain growth in hypoeutectoid Fe–C steels during heating. Acta Materialia 47, 1645-1651.

Karbasian, H., Tekkaya, A.E., 2010. A review on hot stamping. Journal of Materials Processing Technology 210, 2103-2118.

Khaira, H.K., Jena, A.K., Chaturved, M.C., 1993. Effects of heat treatment cycle on equilibrium between ferrite and austenite during intercritical annealing. Materials Science and Engineering A 161, 267-271.

Lenel, U.R., 1983. TTT curves for the formation of austenite. Scripta Metallurgica 17, 471-474.

Li, N., Li, X., Dry, D., Dean, T.A., Lin, J., Balint, D., 2012. Investigation on the mechanical properties of as-formed boron steels for optimizing process strategies in hot stamping, The 14th International Conference of Metal Forming 2012, pp. 1259-1262.

Li, N., Lin, J., Dean, T.A., Dry, D., Balint, D.S., 2014. Concept Validation for Selective Heating and Press Hardening of Automotive Safety Components with Tailored Properties Key Engineering Materials 622-623, 1124-1131.

Liu, F., Sommer, F., Bos, C., Mittemeijer, E.J., 2007. Analysis of solid state phase transformation kinetics: models and recipes. International Materials Reviews 52, 193-212.

Oliveira, F.L.G., Andrade, M.S., Cota, A.B., 2007. Kinetics of austenite formation during continuous heating in a low carbon steel. Materials Characterization 58, 256-261.

Reed, R.C., Akbay, T., Shen, Z., Robinson, J.M., Root, J.H., 1998. Determination of reaustenitisation kinetics in a Fe–0.4C steel using dilatometry and neutron diffraction. Materials Science and Engineering A 256, 152-165.

Roberts, G.A., Mehl, R.F., 1943. The mechanism and the rate of formation of austenite from ferrite-cementite aggregates. ASM Trans. 31, 613 – 650.

Savran, V.I., 2009. Austenite formation in C-Mn steel, Materials Science and Technology. the Delft University of Technology.

Schmidt, E.D., Damm, E.B., Sridhar, S., 2007. A study of diffusion- and interface-controlled migration of the austenite/ferrite front during austenitization of a case-hardenable alloy steel. Metallurgical and Materials Transactions A 38A, 698-715.

Thibaux, P., Tenier, A.M., Xhoffer, C., 2007. Carbon diffusion measurement in austenite in the temperature range 500C to 900C. Metallurgical and Materials Transactions A 38A, 1169-1176.

Thomas, D., Detwiler, D.T., 2009. Microstructural optimization of automotive structures. HONDA MOTOR CO., LTD. (Tokyo, JP), United States.

Yi, J.J., Kim, I.S., Choi, H.S., 1985. Austenitization during intercritical annealing of an Fe-C-Si-Mn dual-phase steel. Metallurgical Transactions A 16A, 1237-1245.

Figure Captions

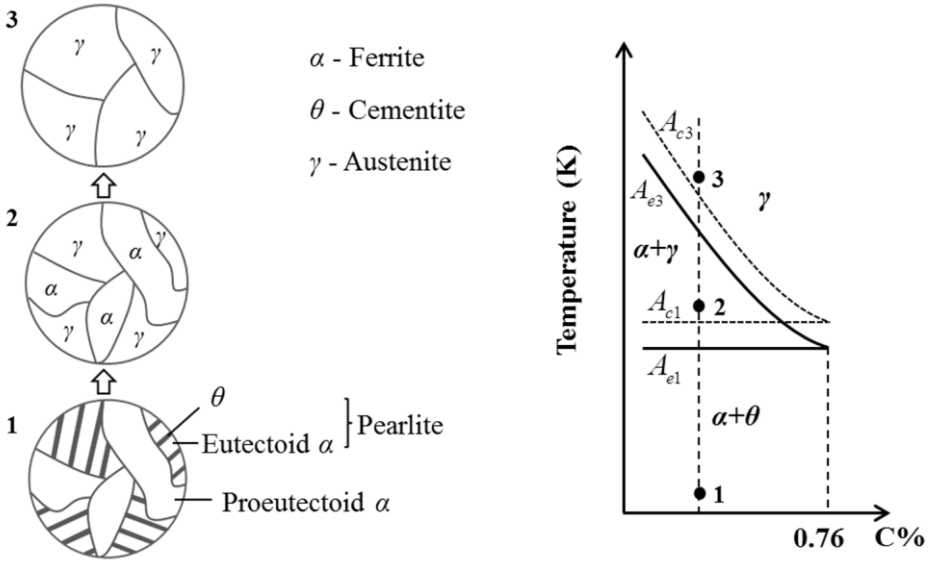

(a) (b)

Figure 1 The formation of austenite in a hypoeutectoid steel (containing less than 0.76wt% C), illustrated by (a) the schematic representations of the microstructure and (b) the evolution in a Fe-C phase diagram (only hypoeutectoid part).

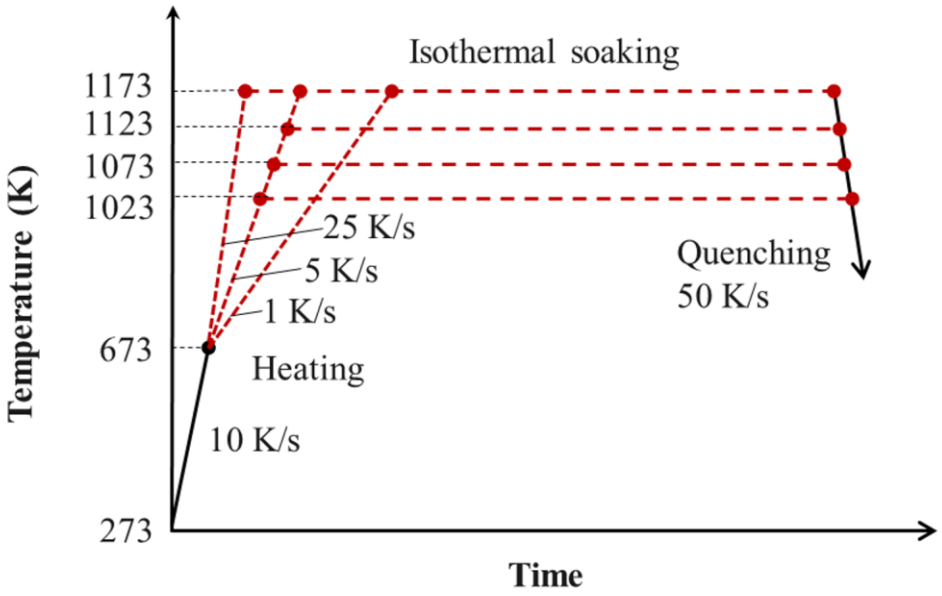

Figure 2 Testing programme with different heating rates (first group) and soaking temperatures (second group).

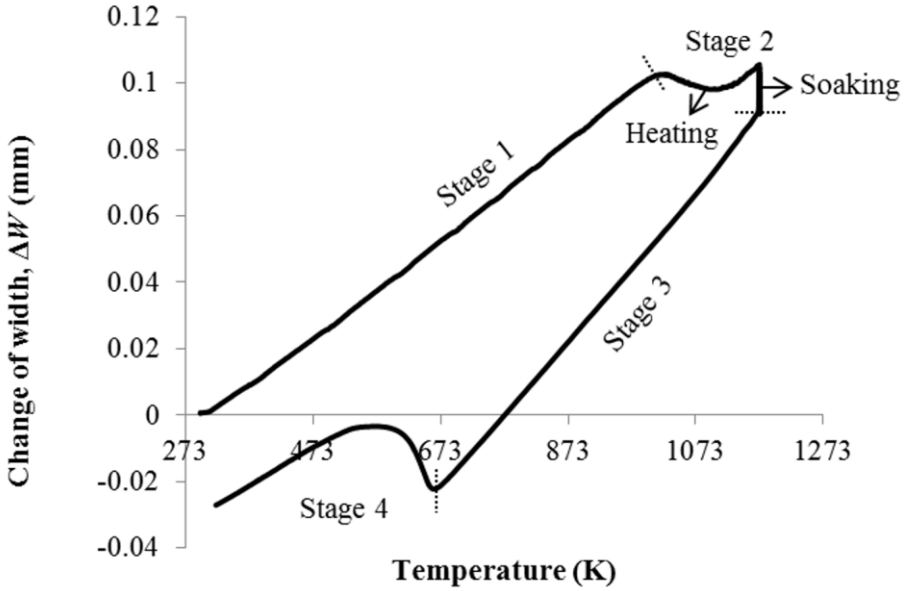

(a) Change of width against temperature

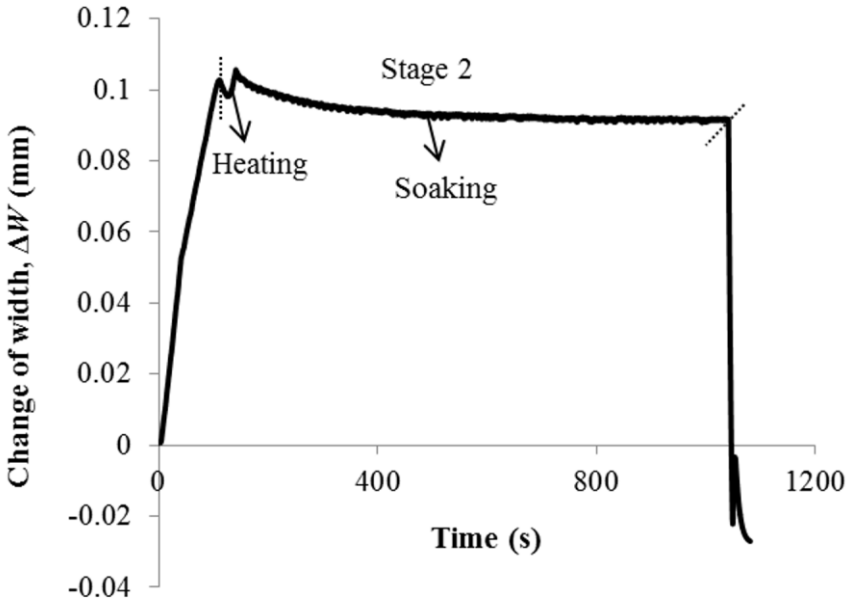

(b) Change of width against time

Figure 3 Experimental curves showing the width change of specimen against (a) temperature and (b) time during the heat treatment process (heating rate: 5K/s, soaking temperature: 1173K).

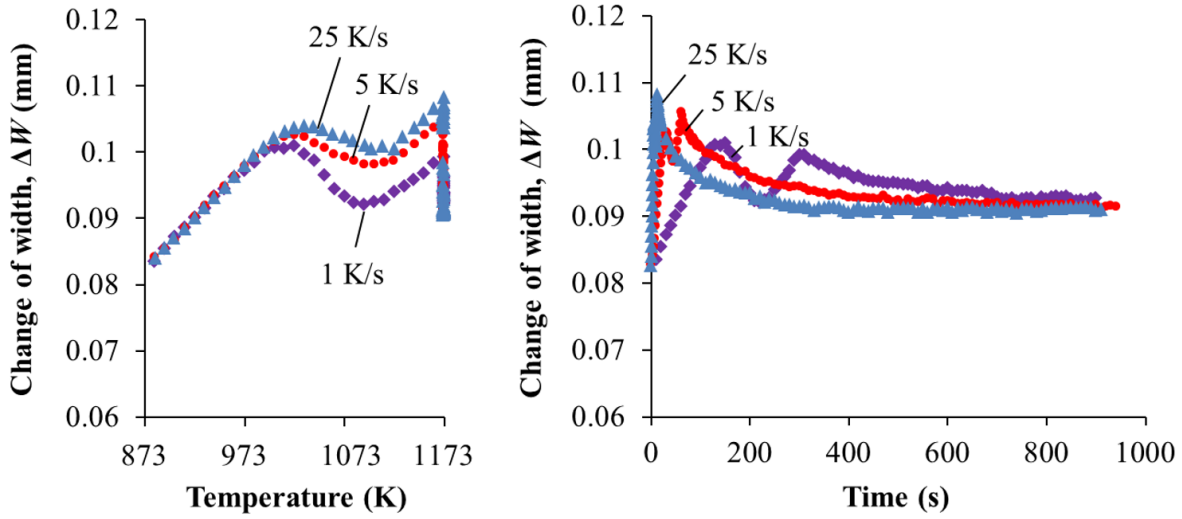

(a) Soaking temperature: 1173K

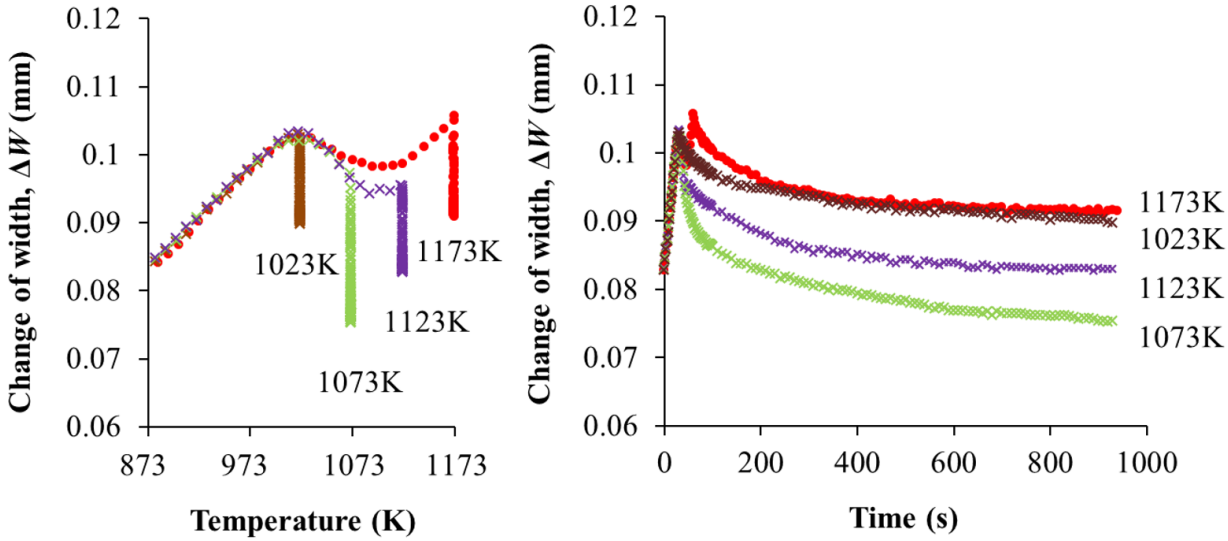

(b) Heating rate: 5K/s

Figure 4 Width changes of specimens tested at different (a) heating rates (soaking temperature: 1173K), and (b) soaking temperatures (heating rate: 5K/s).

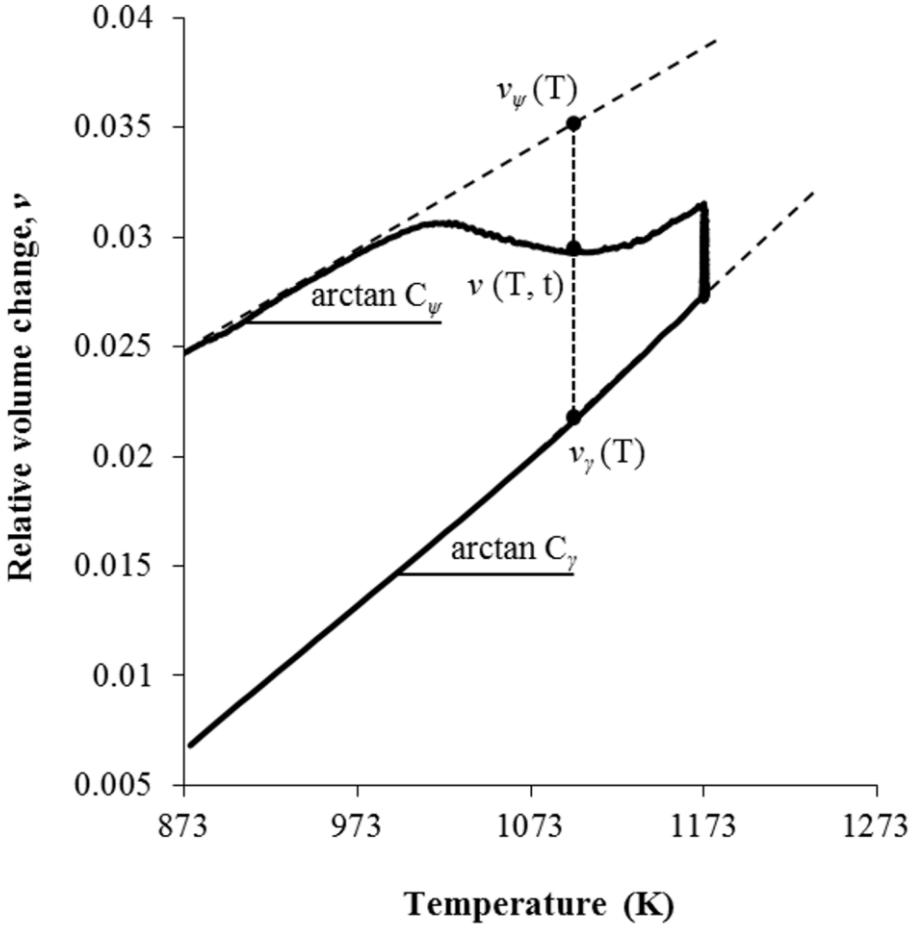

Figure 5 The relation of relative volume change to temperature.

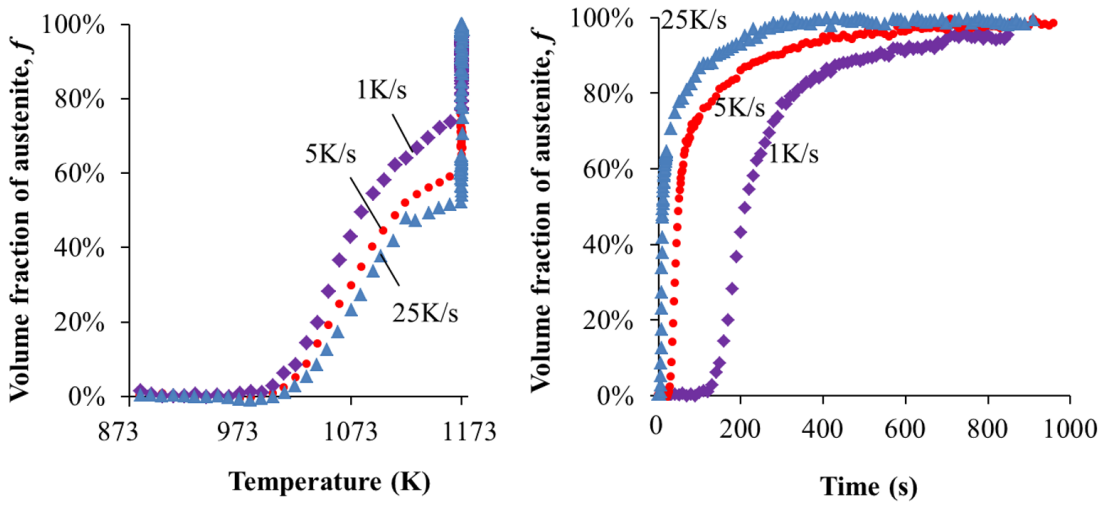

(a) Soaking temperature: 1173K

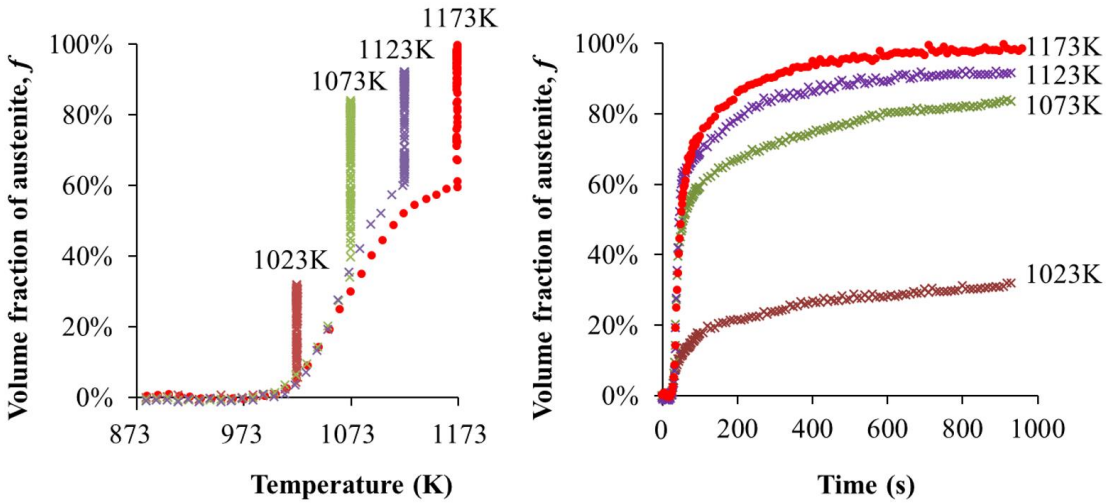

(b) Heating rate: 5K/s

Figure 6 Variation of volume fraction of austenite with temperature and time for different (a) heating rates (soaking temperature: 1173K) and (b) soaking temperatures (heating rate: 5K/s).

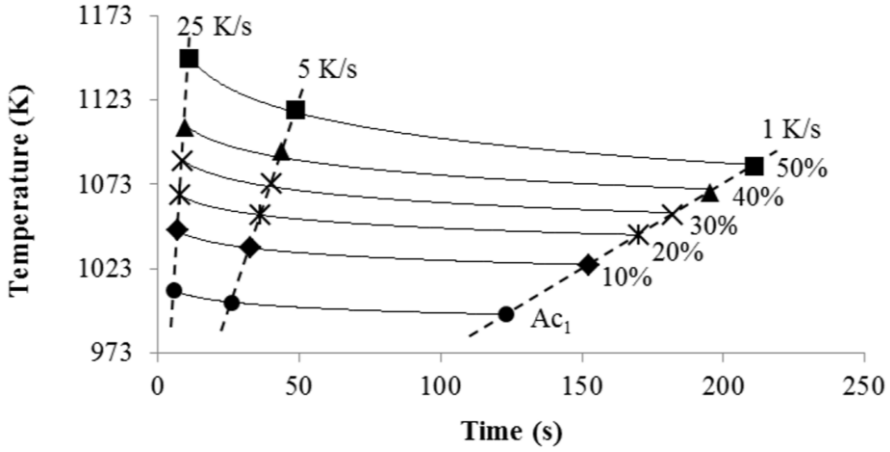

(a) Continuous heating transformation (CHT) diagram

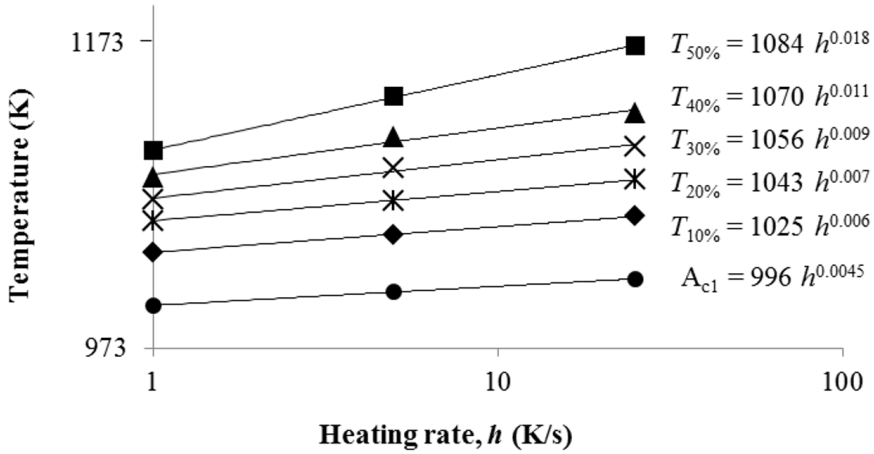

(b) Effect of heating rate on the transformation temperature to attain certain volume fractions of austenite

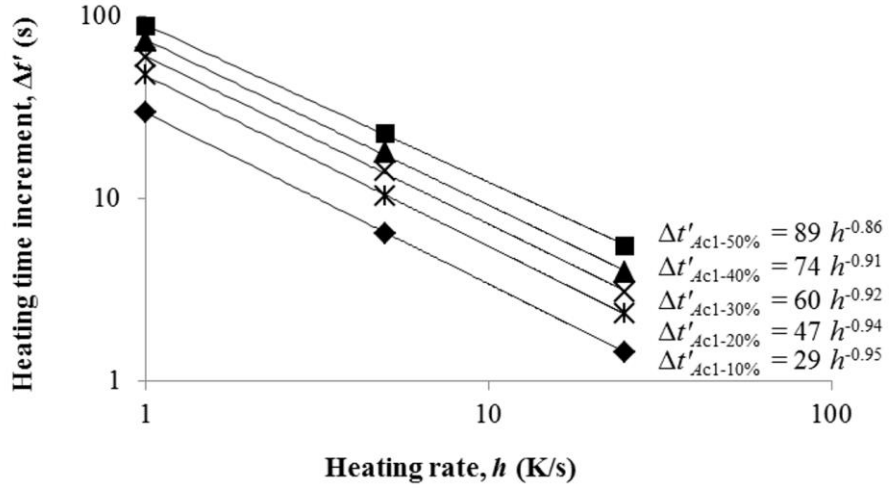

(c) Effect of heating rate on the transformation time to attain certain volume fractions of austenite

Figure 7 Effects of heating rate on austenitization under continuous heating conditions.

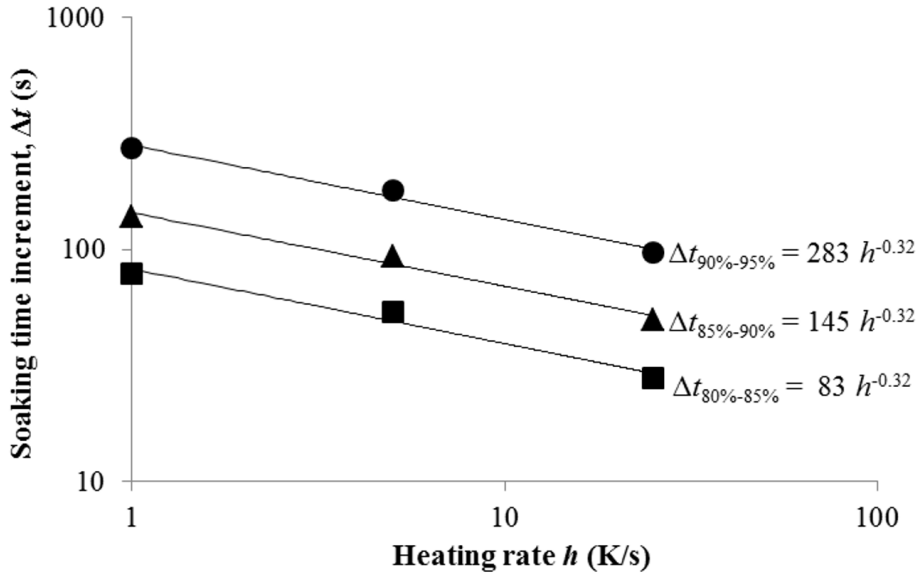

Figure 8 Effect of heating rate on the transformation time to increase austenite volume fraction by 5% from 80%, 85% and 90% during soaking at 1173K.

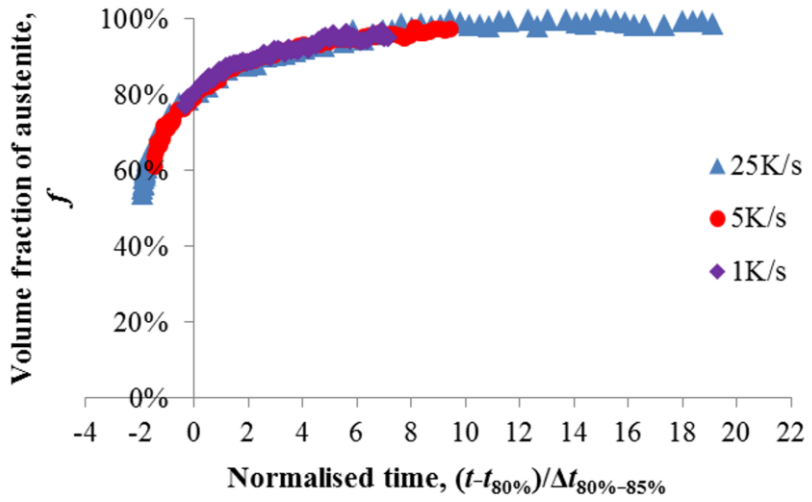

(a) Normalised by $\Delta t_{80\%–85\%}$

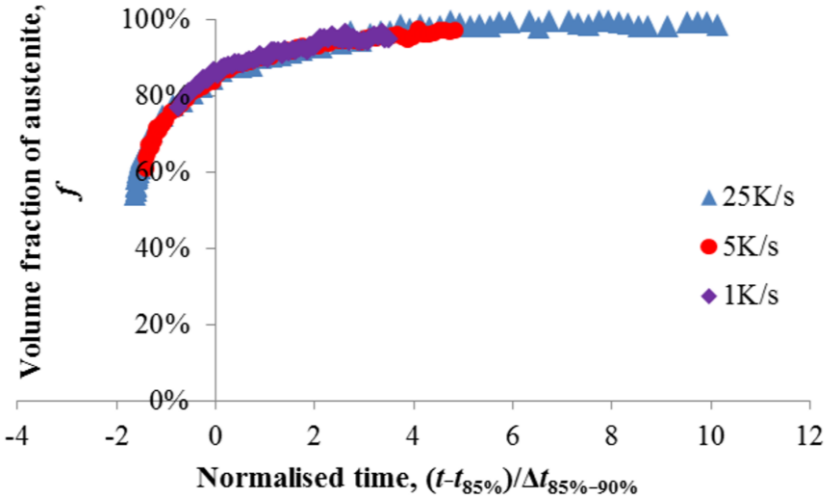

(b) Normalised by $\Delta t_{85\%–90\%}$

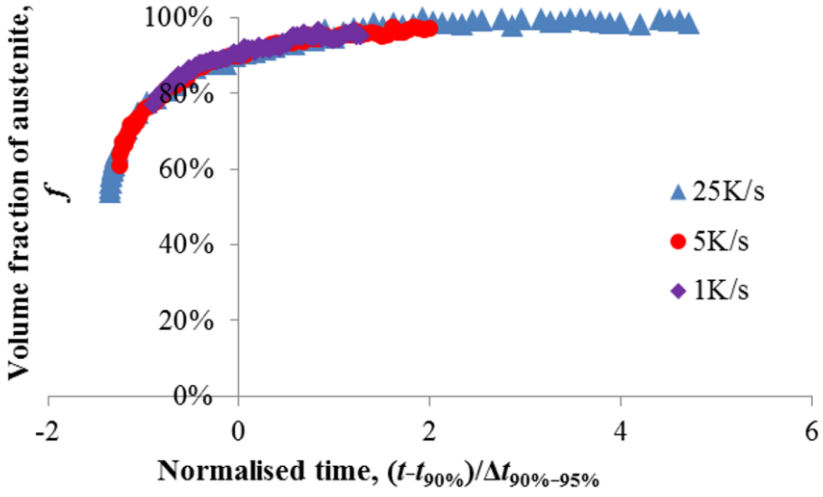

(c) Normalised by $\Delta t_{90\%–95\%}$

Figure 9 Volume fraction of austenite for different heating rates with time normalised by the soaking time increments for different austenite volume fractions, during soaking at 1173K.

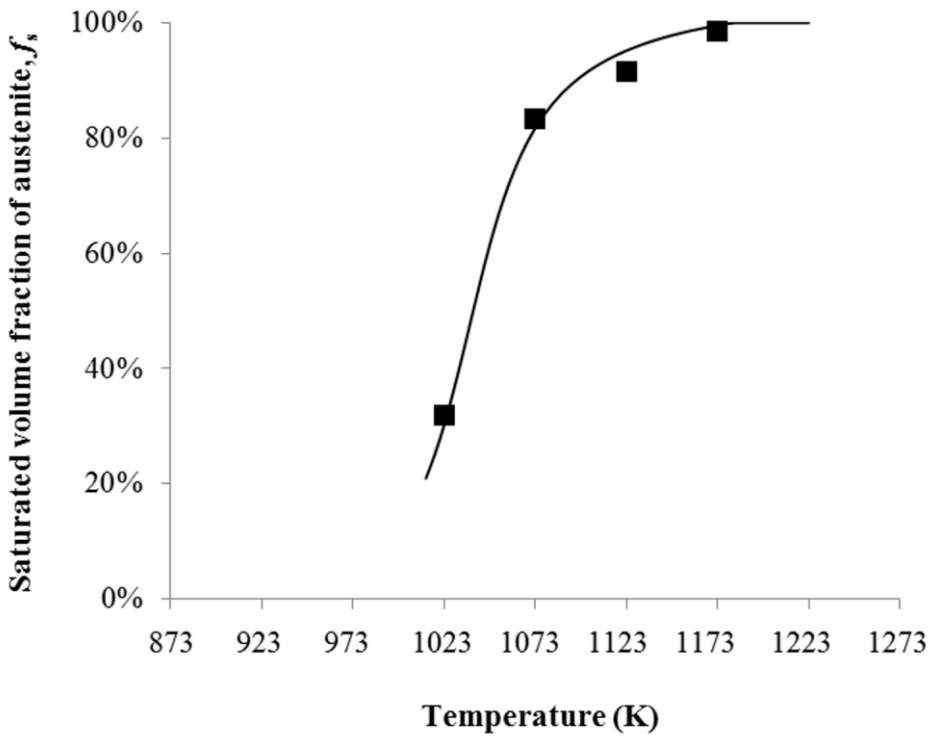

Figure 10 Saturated volume fractions of austenite at different soaking temperatures.

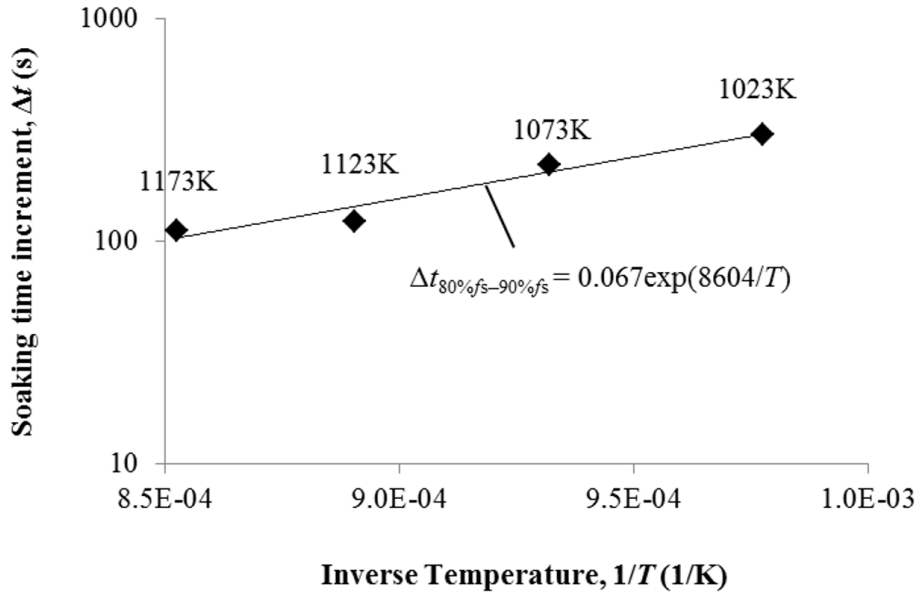

Figure 11 Effect of soaking temperature on the transformation time to increase austenite volume fraction by 10% of f_s from 80% of f_s.

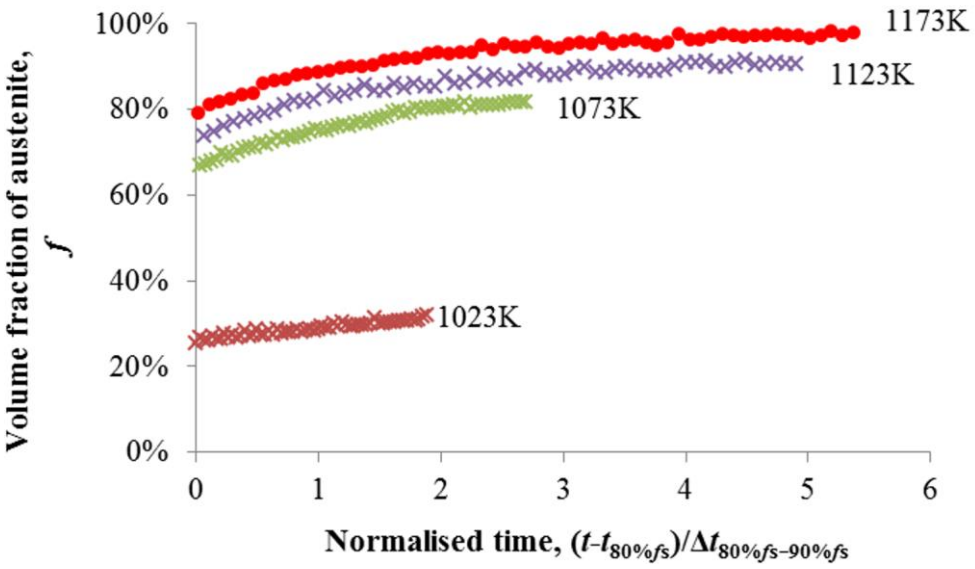

(a) Time is normalised by $\Delta t_{80\%fs–90\%fs}$

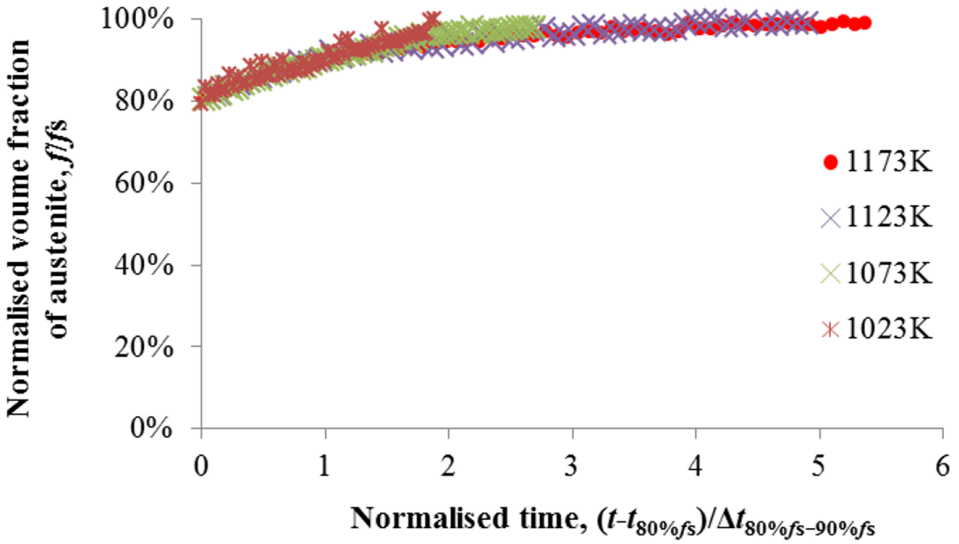

(b) Time is normalised by $\Delta t_{80\%fs–90\%fs}$ and volume fraction of austenite is normalised by f_s

Figure 12 Evolution curves of austenite volume fraction for different soaking temperatures.

Table

Table 1. Chemical composition (Max value - ladle analysis in wt.%).

Steel grade	C	Si	Mn	P	S	Cr + Mo	Ti	B
MBW – K 1500+AS	0.25	0.40	1.40	0.025	0.010	0.50	0.05	0.005